VIP Main-Group Chemistry Very Important Paper

International Edition: DOI: 10.1002/anie.201508670
German Edition: DOI: 10.1002/ange.201508670

The Triboracyclopropenyl Dianion: The Lightest Possible Main-Group-Element Hückel π Aromatic

Thomas Kupfer, Holger Braunschweig, and Krzysztof Radacki*

Abstract: *Hückel π aromaticity is typically a domain of carbon-rich compounds. Only very few analogues with non-carbon frameworks are currently known, all involving the heavier elements. The isolation of the triboracyclopropenyl dianion is presented, a boron-based analogue of the cyclopropenyl cation, which belongs to the prototypical class of Hückel π aromatics. Reduction of Cl_2BNCy_2 by sodium metal produced $[B_3(NCy_2)_3]^{2-}$, which was isolated as its dimeric Na^+ salt ($Na_4[B_3(NCy_2)_3]_2{\cdot}2\,DME$; **1**) in 45 % yield and characterized by single-crystal X-ray diffraction. Cyclic voltammetry measurements established an extremely high oxidation potential for **1** ($E_{pc} = -2.42$ V), which was further confirmed by reactivity studies. The Hückel-type π aromatic character of the $[B_3(NCy_2)_3]^{2-}$ dianion was verified by various theoretical methods, which clearly indicated π aromaticity for the B_3 core of a similar magnitude to that in $[C_3H_3]^+$ and benzene.*

π Electrons have played a crucial role in the development of the aromaticity concept.[1–5] Despite its almost 200 years of history, the fascination with Hückel π aromatics[6,7] has not abated, although cyclically delocalized π systems involving heavier elements have recently shifted into focus with an emphasis on the realization of heavy analogues of the prototypical Hückel π carbocycles (such as $C_3H_3^+$, $C_5H_5^-$, C_6H_6). However, replacement of all ring carbon atoms by other elements with retention of the π electron system is experimentally not trivial, and to date only few species with heteroatom frameworks and classical structures are known. These include 1) the sila- and germaaromatics $[Si_3R_2R']^+$ (R = Si*t*Bu$_3$; R′ = SiMe*t*Bu$_2$), $[Ge_3R_3]^+$ (R = Si*t*Bu$_3$),[8] and $[Si_6Ar_6]$ (Ar = 2,4,6-*i*Pr$_3$C$_6$H$_2$);[9] 2) the non-aromatic cyclobutadiene dianion analogues $[Si_4R_4]^{2-}$ (R = SiMe*t*Bu$_2$), and $[Si_2Ge_2R_4]^{2-}$ (R = SiMe*t*Bu$_2$);[8] 3) the metalloaromatics $[Al_3Ar_3]^{2-}$,[10] $[Ga_3Ar_3]^{2-}$ (Ar = 2,6-(2,4,6-Me$_3$C$_6$H$_2$)C$_6$H$_3$), and $[Ga_4R_2]^{2-}$ (R = Si*t*Bu$_3$);[11] and 4) the aromatic phosphacycles P_5^- and P_6 stabilized by complexation in $[(C_5Me_5)Fe(P_5)]$ and $[\{(C_5Me_5)Mo\}_2(\mu\text{-}P_6)]$.[12]

When it comes to boron, no simple Hückel π system with a pure boron skeleton is currently known, even though boron offers the unique opportunity to study the lighter analogues of the classical organic π aromatics. However, the ability of boron to participate in delocalized aromatic systems either through its empty p orbital (π aromaticity) or its σ bonding scaffold (σ aromaticity) is well-documented. Thus, cyclic delocalization of the π electrons in boracycles such as borirenes (RBC_2R_2), boroles (RBC_4R_4), and borepines (RBC_6R_6) entails classical Hückel π aromatic and antiaromatic structures.[13,14] π Aromaticity was also established theoretically for small inorganic boron rings ($B_3H_n^{+/0/-}$), although in this case the π electrons originate from the σ framework, resulting in non-classical cluster-type structures.[15] The importance of additional σ electron delocalization contributions was emphasized by Berndt and Hofmann for a series of (π + σ) double aromatics with B_3, CB_2, and B_4 skeletons, as well as for some π,σ mixed aromatic boron species, all featuring non-classical bonding situations.[16,17]

We now report the isolation of a boron-based analogue of the classical cyclopropenyl cation (**1**; $Na_4[B_3(NCy_2)_3]_2{\cdot}2\,DME$; Cy = *cyclo*-C$_6H_{11}$; DME = 1,2-dimethoxyethane), a derivative of the aromatic triboracyclopropenyl dianion $[B_3H_3]^{2-}$, which has to be considered the lightest synthetically plausible Hückel 2π aromatic. To this end, the aminoborane Cl_2BNCy_2 was reduced by an excess of sodium sand in DME at room temperature to afford **1** as an orange crystalline solid in 45 % isolated yield (Scheme 1).[18] Formation of **1** was indicated after 5–6 h by the appearance of its characteristic orange–red color, and proceeds quantitatively within 48 h. If high-purity reagents are applied, the reaction is highly selective, and only Cl_2BNCy_2 and **1** are evident in the ^{11}B nuclear magnetic resonance (NMR) spectra of aliquots taken periodically from the reaction mixture. The chemical shift $\delta = 17$ ppm of the broad ^{11}B NMR signal ([D$_8$]THF) is reminiscent of B–B multiple-bond character in **1**, and matches the values found in diborenes[19–21] and diborynes[22] ($\delta \approx 15$–30 ppm).

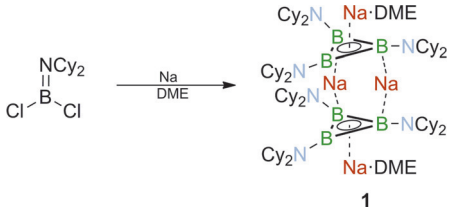

1

Scheme 1. Synthesis of **1** containing the aromatic triboracyclopropenyl dianion $[B_3(NCy_2)_3]^{2-}$.

An X-ray diffraction study on single crystals of **1** (Figure 1)[18] revealed a C_2-symmetric, dimeric structure with inherently planar three-membered B_3 skeletons, and B-B-B angles between 59.6(4)° and 60.3(3)°. The $[B_3(NCy_2)_3]^{2-}$

[*] Dr. T. Kupfer, Prof. Dr. H. Braunschweig, Dr. K. Radacki
Institut für Anorganische Chemie
Julius-Maximilians Universität Würzburg
Am Hubland, 97074 Würzburg (Germany)
E-mail: h.braunschweig@uni-wuerzburg.de

Supporting information for this article is available on the WWW under http://dx.doi.org/10.1002/anie.201508670.

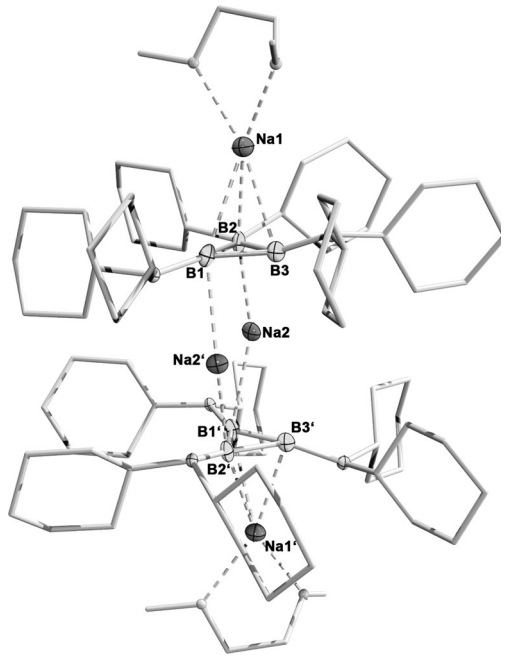

Figure 1. Molecular structure of **1** in the solid state (ellipsoids set at 50% probability). Hydrogen atoms and disorders (cyclohexyl and DME ligands) are omitted for clarity. Selected bond lengths [Å] and angles [°]: B1–B2 1.617(6), B1–B3 1.623(6), B2–B3 1.628(6); B1-B2-B3 60.0(3), B1-B3-B2 59.6(4), B2-B1-B3 60.3(3).

anions are connected by two sodium centers (Na2, Na2′) by electrostatic bonding interactions, which emanate predominately from B1 and B2 (B1–Na2′ 2.561(5) Å, B2–Na2 2.605(5) Å, B3–Na2 2.981(5) Å). A second set of sodium atoms (Na1, Na1′) is located above the other side of the B_3 planes with a more symmetrical coordination mode (Na1–B1 2.675(14) Å, Na1–B2 2.690(15) Å, Na1–B3 2.566(14) Å). The terminal sodium centers Na1/Na1′ are further stabilized by the coordination of the DME oxygen atoms. The presence of two extra electrons within each B_3 core exerts a strong influence on the structural parameters of the $[B_3(NCy_2)_3]^{2-}$ subunits. As the electron density on the boron centers is increased, N→B π bonding contributions become less important, and B–N bonds in **1** (avg. 1.529 Å) are considerably longer than commonly observed (ca. 1.35 Å). More strikingly, the B–B bonds (B1–B2 1.617(6) Å, B1–B3 1.623(6) Å, B2–B3 1.628(6) Å) are shorter than a typical B–B single bond (approx. 1.75 Å), which implies substantial B–B multiple bond character for the $[B_3(NCy_2)_3]^{2-}$ dianion (formal bond order: 1.33). These values might be compared to those found in diborene radical cations (1.63–1.64 Å)[20] and neutral/anionic diborenes (1.56–1.70 Å),[19,21] for which B–B π character and formal bond orders between 1.5 and 2 were established.

Density functional theory (DFT) calculations on fully optimized **1** at the BP86 level of theory (def2-TZVP basis on Na; def2-SVP on H,B,C,N,O) was used to evaluate the electronic structure of the aromatic B_3 three-membered rings.[18] The metrical parameters of $\mathbf{1}^{DFT}$ predicted by DFT (Supporting Information, Figure S7) compare well to those determined experimentally by X-ray diffraction. Inspection of the relevant molecular orbitals (MOs) of $\mathbf{1}^{DFT}$ shows that the highest-occupied molecular orbital (HOMO; orbital 390), and HOMO−1, which accommodate the four extra electrons of the $[B_3(NCy_2)_3]^{2-}$ anions, represent the antisymmetric and symmetric combinations of cyclically delocalized π orbitals of the B_3 core, which is characteristic for classical Hückel π aromatics (Figure 2). Particularly noteworthy is the shape of HOMO−1, which is delocalized over both B_3 subunits spanning the bridging sodium atoms, thus accounting for the stability of the dimeric aggregate. Similar orbital interactions are also observed in typical metallocene systems (for example ferrocene) involving two aromatic ring ligands connected by a central metal atom.

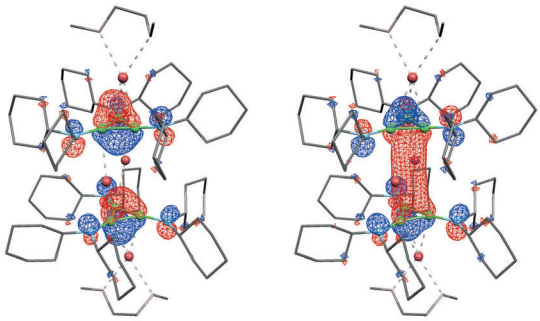

Figure 2. HOMO and HOMO−1 of $\mathbf{1}^{DFT}$ contoured at 0.03 a.u.

The dimeric structure of **1** in the solid state is most likely retained in solution, as deduced from the calculated ^{11}B NMR parameter, taking solvent effects (THF) into account. Thus, a chemical shift of $\delta = 22$ ppm is calculated for the ^{11}B NMR signal of $\mathbf{1}^{DFT}$ (*cf.* **1**: $\delta = 17$ ppm, in [D$_8$]THF), while the isolated $[B_3(NCy_2)_3]^{2-}$ dianion, modeling a solvent-separated ion-pair in solution, shows a ^{11}B NMR resonance shifted downfield at $\delta = 29$ ppm.

A natural bond orbital (NBO) analysis[23] uncovered additional factors contributing to the stability of **1**. The results of the second-order perturbation theory analysis reveal highly stabilizing interactions between the bonding B–B NBOs and 1) the antibonding NBOs of the opposing B–N bonds (45–50 kcal mol^{-1}; for example, BD(B1–B2)→BD*-(B3–N3) 45.49 kcal mol^{-1}), and 2) the empty one-center valence orbitals LP* of the sodium centers (8–10 kcal mol^{-1}). The calculated Wiberg bond indices (WBIs) of the B–B bonds in $\mathbf{1}^{DFT}$ (1.234–1.248) almost match the formal bond order of 1.33, which is in line with substantial B–B multiple bonding within the B_3 skeleton. By contrast, the virtually zero values obtained for the WBIs of the B–Na bonds (0.031–0.036) are indicative of non-covalent, electrostatic bonding interactions.

The electronic structure of **1** was also studied experimentally by cyclic voltammetry (CV) measurements in DME solution using 0.05 M [nBu$_4$N][BAr$^f_4$] (Ar^f = 3,5-(CF$_3$)$_2$-C$_6$H$_3$) as supporting electrolyte.[18] The use of [nBu$_4$N][BAr$^f_4$] was essential to obtain reliable data, as **1** instantaneously reacted with [nBu$_4$N][PF$_6$]. Even PTFE resins are readily defluorinated within seconds when brought into contact with

solutions of **1**. The cyclic voltammogram of **1** shows a single irreversible oxidation event centered at a remarkably negative potential $E_{pc} = -2.42$ V (relative to the ferrocene/ferrocenium couple; Supporting Information, Figure S5). To the best of our knowledge, such a high oxidation potential has never been determined before for any molecular species based on an organic framework.[24,25] Thus, **1** is expected to possess an energetically exceptional high-lying HOMO, which is confirmed by DFT ($E_{HOMO} = -1.85$ eV). For comparison, the strong boron-based reductant I*i*Pr(*i*Pr)B=B(*i*Pr)I*i*Pr (I*i*Pr = 1,3-di-isopropylimidazol-2-ylidene) shows values of $E_{HOMO} = -2.60$ eV (DFT) and $E_{1/2} = -1.95$ V (CV),[21] which fits qualitatively fairly well in this picture.

The high oxidation potential of **1** is also manifest in the reactivity of **1**, which is strongly dominated by redox chemistry. Representative reactions of **1** are depicted in Scheme 2. Thus, $[(i\mathrm{Pr}_3\mathrm{P})_2\mathrm{Pt}^{II}\mathrm{Cl}_2]$ is readily reduced to $[(i\mathrm{Pr}_3\mathrm{P})_2\mathrm{Pt}^{0}]$,[26] and reduction of 1,2-dichloro-1,2-di-*tert*-butyldiborane(4) selectively afforded tetrahedrane **2**.[27]

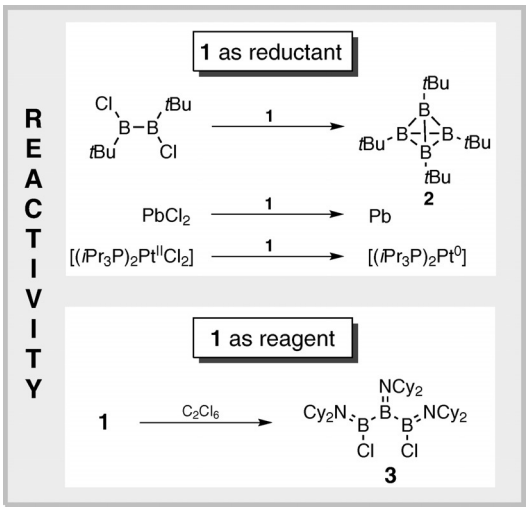

Scheme 2. Reactivity of **1**.

Both transformations are usually a domain of strong alkali-metal-based reductants, and require the use of sodium/naphthalene and Na/K alloy, respectively. Similarly, reaction of **1** with $PbCl_2$ readily yielded elemental lead. However, the nature of the oxidation products of **1** remains unclear. All reactions resulted in an inseparable mixture of different boron-containing species, the main components showing chemical shifts of $\delta = 40$, 45, and 70 ppm in the ^{11}B NMR spectra of the reaction mixtures. These findings compare very well with the results obtained by Baudler et al. for the reduction of Cl_2BNEt_2 with potassium metal in cyclohexane, which afforded a mixture of neutral cycloboranes $B_n(NEt_2)_n$ ($n = 3,4,6$), and octahedral $B_6(NEt_2)_6$ with similar ^{11}B NMR chemical shifts.[28] Here, only the octahedral species was isolated analytically pure, while the cycloboranes were labile and could only be enriched to 57 mol% ($B_3(NEt_2)_3$) and 68 mol% ($B_6(NEt_2)_6$). For instance, $B_3(NEt_2)_3$ readily decomposes to form larger cycloboranes $B_n(NEt_2)_n$. Accordingly, oxidation of **1** presumably involves initial formation of the neutral cyclotriborane $B_3(NCy_2)_3$ and subsequent oligomerization to larger aggregates. All attempts to selectively oxidize **1** with retention of the B_3 three-membered ring have thus far failed. In fact, only oxidation of **1** with C_2Cl_6 in DME showed high selectivity, and afforded a single, well-defined boron-containing product, that is, the triborane **3**. Compound **3** was isolated as a colorless solid in 79% yield, and its molecular structure was validated in the solid state by an X-ray diffraction study (Supporting Information, Figure S6).[18]

Despite its aromatic nature, **1** is not only highly reactive but also rather labile, and it readily decomposes both in solution and in the solid state under ambient conditions within days to unknown colorless decomposition products, which is most likely a consequence of its high oxidation potential in combination with the immense ring strain induced by the rigid B_3 skeletons (**1**: ∢B-B-B: 60° vs. common sp^2 boron: 120°). Even when stored in its crystalline form at −30 °C, initial signs of decomposition are detectable by NMR spectroscopy after 6–7 days. The stability of **1** in solution increased noticeably (2–3 weeks) at low temperatures (−30 °C) if DME is used as the solvent. By contrast, if other donor solvents (tetrahydrofuran, 1-methoxy-2-ethoxyethane, diglyme) or reducing agents are applied, the stability of the aromatic $[B_3(NCy_2)_3]^{2-}$ entity is further reduced. Thus, all attempts to prepare the Li, K, Cs, and Mg congeners of **1** by reduction of Cl_2BNCy_2 with an excess of Li, K, and Cs metal, or Mg(anthracene) were unsuccessful. Here, ^{11}B NMR spectroscopy indicated the formation of species comparable to **1**; however, their low stability prevented any isolation. Obviously, the size of the Na^+ counterions and the coordination of DME are crucial to attain a stable dimeric structure required for the formation of an isolable triboracyclopropenyl dianion derivative.

Using DFT methods (BP86/def2-SVP), we also evaluated the electronic structure and aromaticity of the isolated $[B_3(NCy_2)_3]^{2-}$ dianion (**4**).[18] The calculated geometrical parameters of **4** (Supporting Information, Figure S9) match the experimental values determined for **1** very well, and **4** appears to be suitable to model the electronics of the B_3 framework. The nucleus-independent chemical shift, NICS-(1),[4] calculated 1 Å above the center of the B_3 ring plane of **4** (−13.4 ppm), indicates substantial aromaticity, which is of the same magnitude as values computed (BP86/def2-SVP) for $[C_3H_3]^+$ (−14.1 ppm) and benzene (−10.5 ppm). Similar results are obtained for a commonly used energetic aromaticity descriptor, the aromatic stabilization energy (ASE).[4] Thus, the ASE of **4** ($\Delta E = +31.7$ kcal mol^{-1}; using zero-point corrected energies), estimated according to Equation (1) (Figure 3A), is very similar to that determined for the prototypical Hückel 2π aromatic $[C_3H_3]^+$ ($\Delta E = +29.3$ kcal mol^{-1}), while ring strain effects are negligible here (**4**: $\Delta E_{strain} = -41.9$ kcal mol^{-1}, see Equation (2) in Figure 3A; $[C_3H_3]^+$: $\Delta E_{strain} = -36.9$ kcal mol^{-1}).[15]

The presence of a delocalized π electron system in **4** becomes evident in the analysis of its molecular orbitals. Accordingly, the HOMO of **4** is a π orbital cyclically delocalized over the B_3 skeleton, a situation reminiscent of classical Hückel π aromatics (Figure 3B). By contrast,

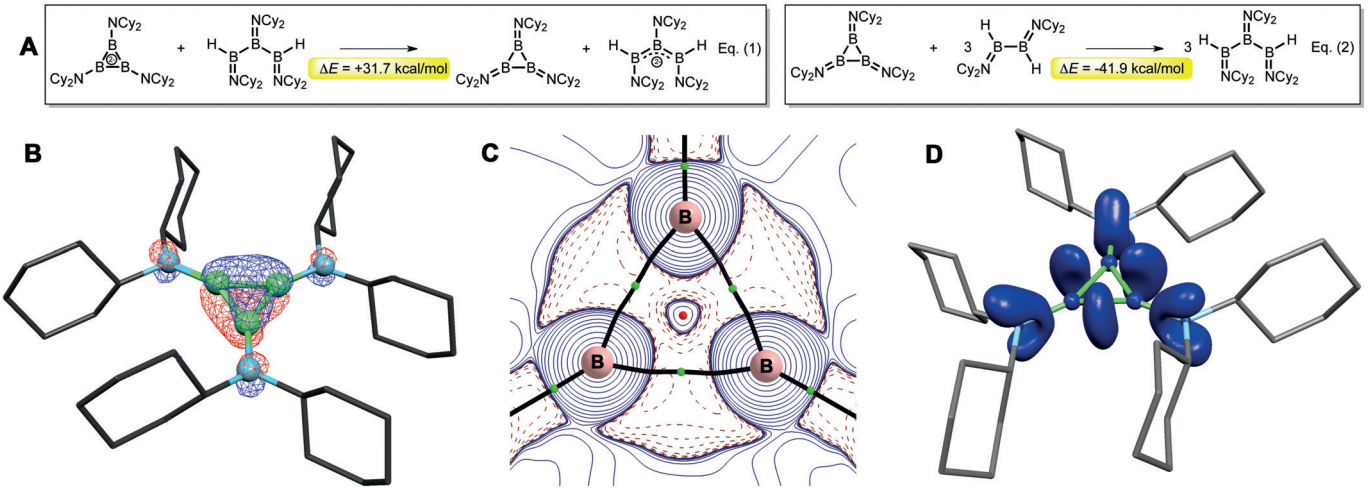

Figure 3. Theoretical bonding analysis of **4**. A) Equations used to estimate the aromatic stabilization energy [ASE; Equation (1)] and ring strain [Equation (2)].[15] B) HOMO of **4** contoured at 0.05 a.u. C) The topology of the Laplacian distribution of charge density in the B_3 plane. Regions of charge depletion are illustrated in solid curves, regions of charge concentration in dashed curves. Bond and ring critical points are also shown. D) Surface of the electron localization function (ELF) contoured at 0.80 a.u. For clarity, only disynaptic valence basins involving boron atoms are shown.

HOMO−1 and HOMO−2 are clearly attributable to the B_3 σ bonding framework (Supporting Information, Figure S10). Furthermore, the topology of the total electron density in **4** was assessed by the atoms-in-molecules (AIM) approach.[29] As expected, bond critical points (BCPs) are present for all B–B bonds with virtually identical electron densities $\rho(r)$ (0.14 a.u.) and strong ellipticities ε (0.38–0.39 a.u.). Furthermore, a ring critical point (RCP) is located at the center of the B_3 ring plane with $\rho(r) = 0.12$. These values compare fairly well with AIM results obtained of $[C_3H_3]^+$ (BCPs: $\rho(r) = 0.21$; $\varepsilon = 0.30$) and benzene (BCPs: $\rho(r) = 0.20$; $\varepsilon = 0.30$). The delocalized bonding situation present in **4** is also illustrated by plotting the Laplacian of the calculated electron density in the plane of the B_3 ring (Figure 3C), which shows an even distribution of the areas of local charge concentration over all atomic basins.

Similarly, analysis of the electron localization function (ELF)[30] computed for the total electrons revealed disynaptic valence basins for B1–B2, B1–B3, and B2–B3 (2.57 electrons (*e*) each) of similar shape (Figure 3D). The most important orbital contributions to V(B1,B2), V(B1,B3), and V(B2,B3) arise from B–B σ [HOMO−1: 0.81/0.05/0.60; HOMO−2: 0.16/0.92/0.38; coefficients in a.u.) and B_3 π bonding interactions (HOMO: 0.40/0.40/0.40). The ELF isosurface of **4** and the occupancy of relevant valence basins strongly resemble the ELF results obtained for $[C_3H_3]^+$ (V(C,C): 2.41 *e* each) and benzene (V(C,C): 2.76 *e* each; Supporting Information, Figure S12), further justifying a description of **1** and **4** as Hückel π aromatic systems.

This work shows that it is possible to realize classical Hückel π systems with frameworks exclusively composed of elements lighter than carbon, that is, based on boron atoms. However, several requirements must be met to attain stable systems. Here, a proper choice of the counterion and solvent, as well as a suitable architecture of the ligand scaffold for kinetic stabilization reasons, were essential for the isolation of $Na_4[B_3(NCy_2)_3]_2{\cdot}2\,DME$ containing the $[B_3(NCy_2)_3]^{2-}$ dianion. As established by density functional theory, $[B_3(NCy_2)_3]^{2-}$ is a true Hückel aromatic with a π electron system cyclically delocalized over the B_3 three-membered ring. Accordingly, $Na_4[B_3(NCy_2)_3]_2{\cdot}2\,DME$ has to be considered the lightest possible Hückel π aromatic accessible experimentally.

Keywords: aromaticity · boron · density functional therory · multiple bonding

How to cite: *Angew. Chem. Int. Ed.* **2015**, *54*, 15084–15088
Angew. Chem. **2015**, *127*, 15299–15303

[1] A. T. Balaban, P. von R. Schleyer, H. S. Rzepa, *Chem. Rev.* **2005**, *105*, 3436.
[2] P. von R. Schleyer, H. Jiao, *Pure Appl. Chem.* **1996**, *68*, 209.
[3] M. Randić, *Chem. Rev.* **2003**, *103*, 3449.
[4] Z. Chen, C. S. Wannere, C. Corminboeuf, R. Puchta, P. von R. Schleyer, *Chem. Rev.* **2005**, *105*, 2842.
[5] T. M. Krygowski, H. Szatylowicz, O. A. Stasyuk, J. Dominikowska, M. Palusiak, *Chem. Rev.* **2014**, *114*, 6383.
[6] E. Hückel, *Z. Phys.* **1931**, *70*, 204.
[7] E. Hückel, *Grundzüge der Theorie ungesättigter und aromatischer Verbindungen*, Verlag Chemie, Berlin, **1940**.
[8] V. Y. Lee, A. Sekiguchi, *Angew. Chem. Int. Ed.* **2007**, *46*, 6596; *Angew. Chem.* **2007**, *119*, 6716.
[9] K. Abersfelder, A. J. P. White, H. S. Rzepa, D. Scheschkewitz, *Science* **2010**, *327*, 564.
[10] R. J. Wright, M. Brynda, P. P. Power, *Angew. Chem. Int. Ed.* **2006**, *45*, 5953; *Angew. Chem.* **2006**, *118*, 6099.
[11] Y. Wang, G. H. Robinson, *Organometallics* **2007**, *26*, 2.
[12] L. Nyulászi, *Chem. Rev.* **2001**, *101*, 1229.
[13] J. J. Eisch, *Adv. Organomet. Chem.* **1996**, *39*, 355.
[14] H. Braunschweig, T. Kupfer, *Chem. Commun.* **2011**, *47*, 10903.
[15] A. A. Korkin, P. von R. Schleyer, M. L. McKee, *Inorg. Chem.* **1995**, *34*, 961.

[16] W. Mesbah, C. Präsang, M. Hofmann, G. Geiseler, W. Massa, A. Berndt, *Angew. Chem. Int. Ed.* **2003**, *42*, 1717; *Angew. Chem.* **2003**, *115*, 1758.
[17] M. Hofmann, A. Berndt, *Heteroat. Chem.* **2006**, *17*, 224.
[18] Experimental, spectroscopic, crystallographic, and computational details are given in the Supporting Information. CCDC 1413704 (**1**) and 1413705 (**3**) contain the supplementary crystallographic data for this paper. These data can be obtained free of charge from The Cambridge Crystallographic Data Centre.
[19] P. Bissinger, H. Braunschweig, A. Damme, T. Kupfer, A. Vargas, *Angew. Chem. Int. Ed.* **2012**, *51*, 9931; *Angew. Chem.* **2012**, *124*, 10069.
[20] P. Bissinger, H. Braunschweig, A. Damme, I. Krummenacher, T. Kupfer, A. Vargas, *Angew. Chem. Int. Ed.* **2014**, *53*, 5689; *Angew. Chem.* **2014**, *126*, 5797.
[21] P. Bissinger, H. Braunschweig, A. Damme, C. Hörl, I. Krummenacher, T. Kupfer, *Angew. Chem. Int. Ed.* **2015**, *54*, 359; *Angew. Chem.* **2015**, *127*, 366.
[22] H. Braunschweig, R. D. Dewhurst, K. Hammond, J. Mies, K. Radacki, A. Vargas, *Science* **2012**, *336*, 1420.
[23] NBO 6.0, Theoretical Chemistry Institute, University of Wisconsin, Madison, **2013**.
[24] H. S. Farwaha, G. Bucher, J. A. Murphy, *Org. Biomol. Chem.* **2013**, *11*, 8073.
[25] N. G. Connelly, W. E. Geiger, *Chem. Rev.* **1996**, *96*, 877.
[26] A. Nova, S. Erhardt, N. A. Jasim, R. N. Perutz, S. A. Macgregor, J. E. McGrady, A. C. Whitwood, *J. Am. Chem. Soc.* **2008**, *130*, 15499.
[27] T. Mennekes, P. Paetzold, R. Boese, D. Bläser, *Angew. Chem. Int. Ed. Engl.* **1991**, *30*, 173; *Angew. Chem.* **1991**, *103*, 199.
[28] M. Baudler, K. Rockstein, W. Oehlert, *Chem. Ber.* **1991**, *124*, 1149.
[29] R. F. W. Bader, *Atoms in Molecules: A Quantum Theory*, Oxford University Press, Oxford, **1990**.
[30] A. Savin, O. Jespen, J. Flad, O. K. Anderson, H. Preuss, H. G. von Schnering, *Angew. Chem. Int. Ed. Engl.* **1992**, *31*, 187; *Angew. Chem.* **1992**, *104*, 186.

Received: September 16, 2015
Published online: November 4, 2015

